The effect of alloying additions on the structure and properties of Al-Mg-Si-Mn casting alloy – A review

Viktoriya Boyko[1] iD , Edward Czekaj[2] iD , Małgorzata Warmuzek[2] iD , Kostiantyn Mykhalenkov[1]* iD

[1]National Technical University of Ukraine "Igor Sikorsky Kyiv Polytechnic Institute", Prospect Pobedy 37, Kiev, Ukraine
[2]ŁUKASIEWICZ – Foundry Research Institute, ul. Zakopiańska 73, 30-418 Krakow, Poland

*Corresponding author: kvmykhalenkov@gmail.com

Abstract

The designing of new light-weight alloys for continuous replacement of cast iron and steel parts is now the mainstream regarding energy saving and improvement of fuel consumption in the transportation sector. Parallel with the remarkable advances in aluminium wrought alloys, the search for novel efficient casting alloys still attracts the attention of researchers and manufacturers of aluminium casting. The last decades have shown a growing interest in Al-Mg-Si-Mn casting alloys. Despite their active implementation into foundry practice, there is a lack of research regarding their structural formation after additional alloying by Cu, Zn, Sc, Zr, Ti, Li, and especially the effect of 'natural hardening' when an alloy undergoes aging from as-cast condition. In this paper the authors have summarised the existing information on the Al-Mg-Si-Mn casting alloys, including their structure and the effects of Mn, Cu, Zn, Sc, Sc+Zr and Li additions on the properties, along with their own results concerning this group of casting materials.

Keywords: *aluminium alloys, casting, Al-Mg-Si system, alloying addition, precipitation*

1. Introduction

Simultaneously, with the progress in the designing of efficient Al-Si casting alloys, another group of materials has undergone its wide implementation into foundry practice. These are the alloys of Al-Mg-Si-Mn system containing in the range of (wt.%): 5.0−5.5 Mg, 1.5−2.2 Si, and Mn 0.6 wt.%. It has been shown by many researchers that such composition of an alloy subjected to high pressure die casting (HPDC) gives certain advantages of the cast parts in comparison to well established commercial alloys of the Al-Si system [1]. The attractiveness of these alloys is based on the combination of intermediate strength with high ductility. This is of great importance for the design of novel effective light-weight automotive body structures.

An explanation of this statement can be made. Available commercial Al-Mg-Si wrought alloys used in the car-building industry, such as 6016, 6009 or 6010 in heat treated condition (T6 or T4) possess the mechanical properties in the range of 120 to 220 MPa of yield strength (YS), 220−290 MPa of the ultimate tensile strength (UTS), and 24−25% of elongation to fracture [2,3]. In order to maximize the benefits of an aluminium-intensive car body structure, the die-castings need to have comparable mechanical properties with the components made of aluminium sheets or extrusions. However, the mechanical properties of currently available die-cast alloys are not competitive and cannot satisfy the industrial requirements. In particular, the ductility is not sufficient in manufacturing and in the application [3]. Therefore, the cast alloy needs to be specially developed for car body structures and similar applications where elongation is one of the crucial characteristics.

Currently, the die-cast aluminium alloys include Al-Si-Cu, Al-Si and Al-Mg-Si and Al-Mg. Al-Si-Cu (AlSi9Cu3(Fe)) and Al-Si alloys are the most popular alloys that offer a good combination of strength, castability and processability, but less ductility. As an example, it was reported by Sanna et al. [4] that the alloy AlSi9Cu3(Fe) (subjected to HPDC) showed the elongation to fracture on the level of 2−5%. Simultaneously, the Al-Mg-Si-Mn alloy can provide a much higher ductility of 15−18% that is approximately three times higher than that of AlSi9Cu3 together with similar UTS of 300 MPa [3,45]. The specification of available Al-Mg-Si-Mn die-cast alloys varies throughout different countries and manufacturers. It has been summarised by Boyko et al. [1] and Ji et al. [3] together with advantages of this group of casting alloys:

a) high mechanical properties;

b) good fluidity, which provides the Al-Mg-Si casting alloys the ability to fill the thinnest sections of a mould cavity;

c) good feeding behaviour;

d) good corrosion resistance and stress corrosion cracking.

The main reason behind the design of this material was the necessity to combine the superior mechanical properties of the Al-Mg system with its application in high pressure die-casting (HPDC). According to the concept of alloy design [5,6], the main alloying elements are magnesium, silicon, and manganese.

Magnesium goes into solution and results in high YS by forming coherent and semi-coherent phases in the α-Al. The ratio of magnesium to silicon is also very important for achieving the desired 40−50% eutectic volume fraction. This in turn favours sufficient castability and feeding during solidification. No free silicon must be available in order to provide outstanding corrosion behaviour [5]. The last requirement is somewhat controversial because, in the absence of silicon, there are no building materials for precipitates to form on, and subsequently, the matrix will be strengthened only by the solid solution mechanism.

It is well known that the mechanical properties of an alloy with nominal composition AlMg5Si2Mn strongly depends on the wall thickness of the cast part. For 2−3 mm wall thickness, UTS can reach 330 MPa, YS 220 MPa, 18% elongation. Further enlargement of wall thickness leads to a dramatic decrease of all characteristics [5]. It was also detected that the UTS and YS vary with applied casting techniques. The highest values can be achieved for HPDC and lowest for permanent mould (PM) casting [46].

To improve mechanical properties, the authors [3] optimised the Mg content in the AlMg5Si2Mn alloy. They showed that the maximum UTS and YS can be achieved at 5.50 wt.%. Further improvements of mechanical properties were possible by additional alloying. For this purpose, Zn, Cu, Ti, Sc, Zr were applied and a brief summary of the results can be found in the recent work of Boyko et al. [1]. However, the effect of different alloying additions on the structure formation, precipitation processes and the resulting mechanical properties is not completely understood. Therefore, the main objective of the present paper is to show the role of different alloying elements on the structure and precipitation of strengthening phases in Al-Mg-Si-Mn casting alloys, based on previously published works [1,7,9,12,44] and the available literature on the subject [4,10,11,13,16,18,20−23,35,43].

2. Effect of alloying elements

2.1. Effect of Mg and Si

The major alloying elements in Al-Mg-Si alloys are Mg and Si. The temperature of the α-Al + Mg$_2$Si pseudobinary eutectic solidification was 594°C [8], which is in the agreement with differential scanning calorimetry (DSC) measurements performed by Mykhalenkov K. et al. [9]. DSC results (Fig. 1a) demonstrated the eutectic melting temperature to be 594°C (Fig. 1a). This is one of the highest eutectic melting temperatures for Al-based alloys. The calculated chemical composition of the phases taking part in eutectic reaction is listed in Table 1 [8].

Table 1. Invariant equilibria of Al-Mg-Si system [8]

Reaction	T, °C	Phase	Composition, at.%/wt.%		
			Al	Mg	Si
L ⇆ α-Al + Mg$_2$Si	594	L	85.30/86.08	10.80/9.82	3.9/4.10
		α-Al	97.10/97.35	2.70/2.44	0.2/0.21
		Mg$_2$Si	0	66.70	33.30

By using transmission electron microscopy and EDX microanalysis performed across and along the dendrite arms in AlMg5.3Si1.8Mn0.62 alloy, it was found [7] that at room temperature the average Mg content in the α-Al solid solution was about 2.20 wt.% (*see* Table 2). Simultaneously, the Si content was found to be lower than the limit of detection for EDS microanalysis, i.e. 0.1 wt.%. Therefore, almost all Si was built to the Mg$_2$Si eutectic lamella, and some into AlFeMnSi intermetallic phase. The solid solution was saturated with Mg.

The composition of α-Al estimated in TEM+EDX, using spot size down to 0.8 nm, showed a Mg content in the range of 2.20−2.30 wt.% for alloy cast into permanent mould and for AlMg5.47Si2.20Mn0.69 HPDC alloy. In the latter case, the cooling rate is one order higher (about of 70 K·s^{-1}). Thus, the Mg supersaturation of the α-Al solid solution was almost independent of the casting techniques used (Table 2). An increase in the cooling rate cannot increase the saturation of the α-Al with other alloying elements Mn and Si.

The difference of the UTS, YS, and elongation between both alloys (one cast into permanent mould (PM) and the second HPDC), was usually attributed to the following factors:

– smaller size of the α-Al grains of the HPDC alloy than those of the PM;

– changes of the eutectic morphology from plate-like to fibrous;

– formation of large shrinkage pores in the PM alloy.

Table 2. Chemical composition of α-Al in AlMgSiMn alloy as affected by cooling rate

Element	Alloy			
	Casting PM		Casting HPDC	
	SEM, wt.%	TEM, wt.%	SEM, wt.%	TEM, wt.%
Mg	2.6	2.2	2.8	2.4
Si	0.3	–	0.3	–
Mn	0.4	0.5	0.5	0.5

Ji et al. [3] reported that the maximum UTS was obtained for an alloy, containing as much as 8.80 wt.% Mg, and it was constantly increasing with the increasing addition of Mg. However, the elongation of the alloy with such a high Mg content drastically decreased from 17% down to 8% in comparison to the alloy containing 5.50 wt.% Mg and 1.50 wt.% Si. Therefore, to satisfy the demand for high plasticity, the optimum composition of an alloy was proposed: 5.00−5.50 wt.% Mg and 1.50−2.00 wt.% Si.

The average elements content in Mg_2Si eutectic lamella was: Mg – 18.30 wt.%; Si – 34.10 wt.%, Al – 18.70 wt.%. Beside the matrix effect (Al presence), the spectra showed relatively high oxygen content of 28 wt.%. This result suggests that eutectic lamellae of Mg_2Si exhibits a strong tendency for oxidising. However, some results obtained through TEM/EDS microanalysis allowed the estimation of the composition of Mg_2Si particles of Mg/Si ratio near their stoichiometry: Mg – 64.6 at.%, Si – 31.2 at.%, other (O, Fe, Cu, Zn, Al) – 4.2 at.%.

2.2. Effect of Mn

One of the reasons for adding Mn to Al-based casting alloy is to alter the morphology of the Fe-bearing phase by promoting the formation of compact α-AlFeMnSi intermetallic particles [3] instead of needle shaped AlFeSi phase. It is also claimed that the Mn content has a low effect on the mechanical properties, and its addition is usually kept on the level of 0.60 wt.% [3,10] to prevent die soldering.

In the AlMg5.3Si1.8Mn0.62 alloy cast into permanent mould, it was found that the Mn mostly dissolved in the Al matrix. The distribution of Mn across the dendrite arm in AlMg5.47Si2.20Mn0.69 HPDC alloy is represented in Figure 1d. One can see that the Mn is almost evenly distributed in the α-Al on the level of 0.45−0.50 wt.%. However, primary particles of the α-Al(Mn,Fe)Si phase were revealed in the inter-dendritic eutectic. Morphology of Mn-containing primary phase is shown on Figure 2a. Its chemical composition is (in at.%): Al – 74.5, Mn – 15.8, Si – 4.7, Fe – 0.1.

In the alloy subjected to heat treatment, the primary α-Al(Mn,Fe)Si particles dissolved during homogenisation. In the areas of the solid solution, new precipitates

containing Mn were observed. The preferential morphology of these particles is block-like and they are randomly distributed in the matrix. During prolonged annealing, the size and volume fraction of these particles become larger [1]. The precipitated dispersoids mainly contained Mn, Si, and Al. In some cases, small concentrations of Mg were detected. The measured Fe content was not greater than 0.70 wt.%. The chemical composition and morphology of the observed dispersoids allow the identification of them as an α-Al(Mn,Fe)Si phase.

The appearance of these α-Al(Mn,Fe)Si dispersoids proves the dual effect of Mn addition namely: (i) formation of the primary α-Al(Mn,Fe)Si inter-metallics during solidification; (ii) the reprecipitation of the dispersive, Mn-rich phase during the solution treatment contributing into a precipitation strengthening effect.

2.3. Effect of the zebra-crossing precipitates

TEM investigations performed on a series of Al-Mg-Si-Mn casting alloys cast into permanent mould (as well as HPDC) showed that the α-Al grains contain plate-like precipitates [1,7,9]. These plates are elongated along a certain direction and are arranged parallel to each other, resulting in a pattern like a zebra crossing (as can be seen on Fig. 3). On one side of this pattern, a carved black line is visible, which could be identified as a dislocation. This generalization is true for all of the studied alloys.

Detailed investigations of these precipitates allowed to reveal their features:

– composition of precipitates is very close to stoichiometric Mg_2Si compounds;

– precipitates are aligned along dislocations, for all specimens;

– precipitation density is much higher for the HPDC alloy than for the PM alloys;

– precipitates are only distributed in the α-Al solid solution dendrites – they were not detected in the α-Al eutectic lamellas.

From this observation, together with the revealed alignment of precipitates along the dislocations, it can be concluded that the main mechanism of their formation is the heterogeneous nucleation in the stress field of dislocations during the natural aging of the alloy. The high dislocation density in the HPDC alloy originated from differences in the thermal expansion of α-Al and Mg_2Si, together with the pressure applied during HPDC, which provided more nucleation sites for the precipitates.
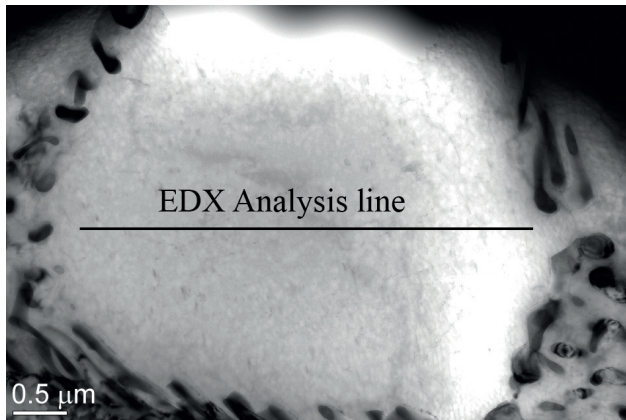
These results clearly indicate that one of the main origins of high mechanical properties of an Al-Mg-Si-Mn HPDC alloy is the precipitation of strengthening phases
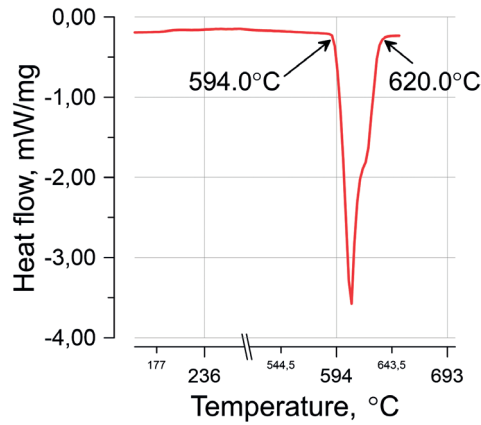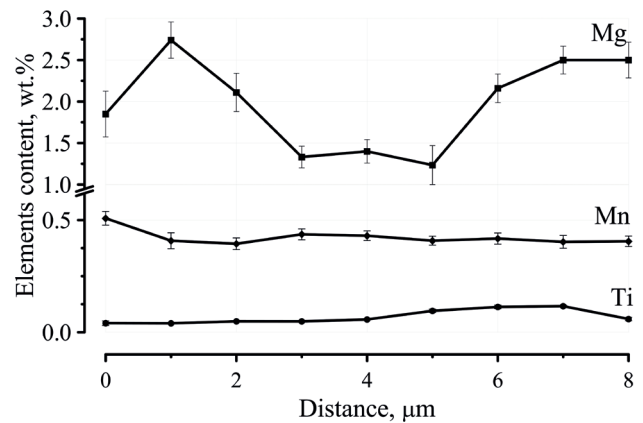
a) DSC traces of AlMg5.5Si2.1 alloy
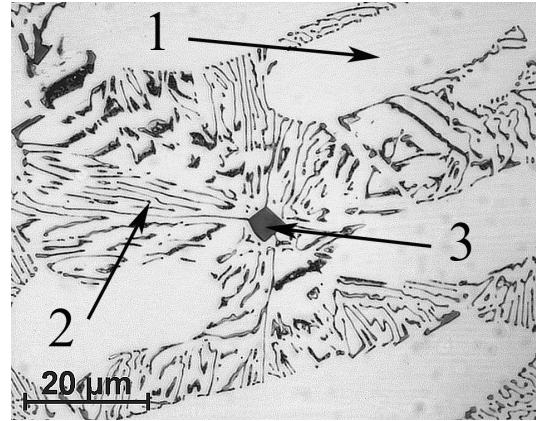
b) Microstructure of AlMg5.5Si2.1 alloy
1 – α-Al solid solution, 2 – (α-Al) + (Mg₂Si) eutectic,
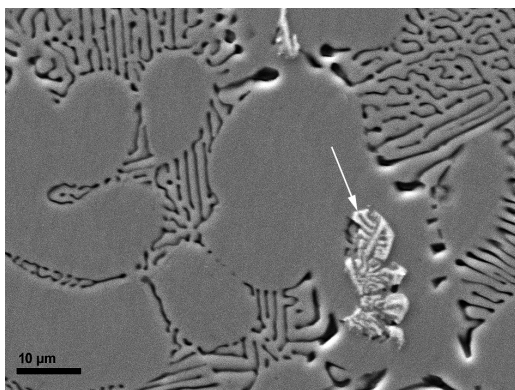*3 – primary Mg₂Si crystal*

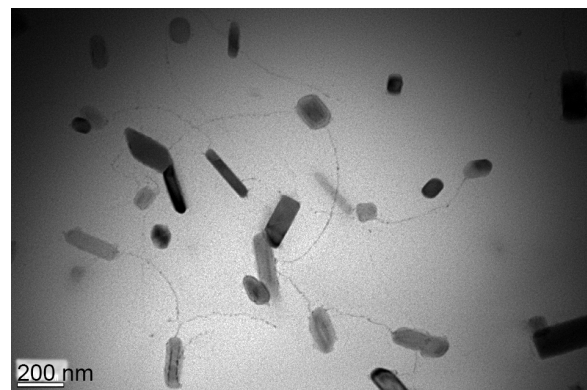*c) Line of EDX microanalysis of AlMg5.47Si2.20Mn0.69 HPDC alloy*

d) Distribution of Mg, Mn and Ti across dendrite arm along line marked in Fig. 1c

Fig. 1. DSC traces (a), microstructure (b) and alloy components distribution (c,d) [9] in AlMg5.47Si2.20Mn0.69 alloy

a) Morphology of Mn-containing phase in AlMg5.70Si1.85Mn0.61 alloy cast into permanent mould (marked by arrow)

b) Bright field image of Mn-containing precipitates in the AlMg5.70Si1.85Mn0.61 alloy cast into permanent mould. Alloy was heat treated at 570°C for 1 hour, quenched into water and artificially aged at 175°C for 60 min

Fig. 2. Morphology of primary α-Al(Mn,Fe)Si phase in AlMg5.70Si1.85Mn0.61 alloy cast into permanent mould (a) and dispersive Mn-containing precipitates observed in the alloy after heat treatment (b)
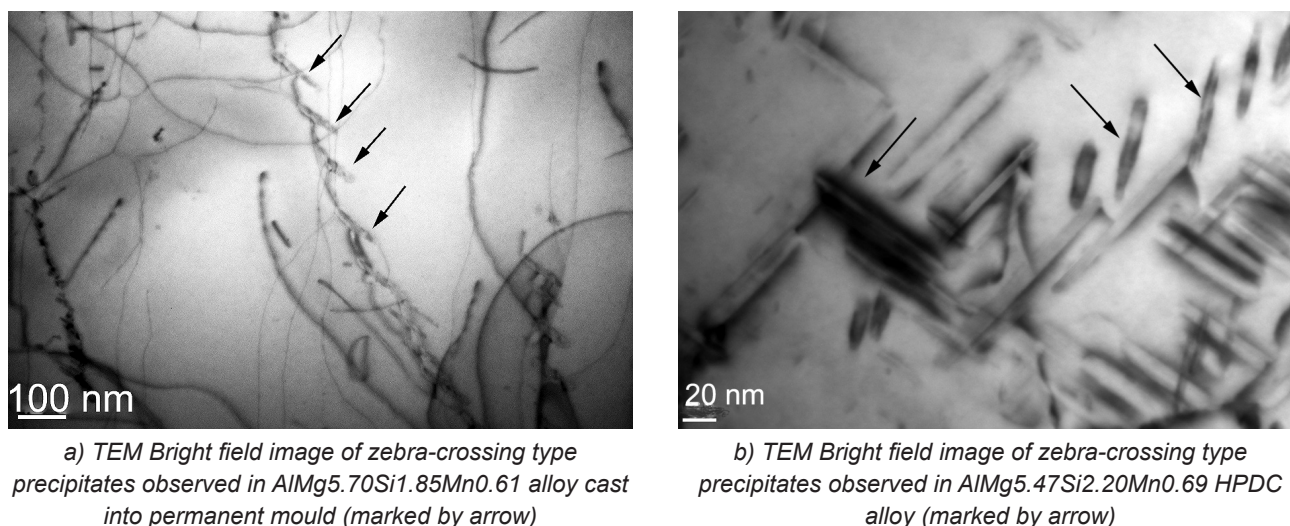
a) TEM Bright field image of zebra-crossing type precipitates observed in AlMg5.70Si1.85Mn0.61 alloy cast into permanent mould (marked by arrow)

b) TEM Bright field image of zebra-crossing type precipitates observed in AlMg5.47Si2.20Mn0.69 HPDC alloy (marked by arrow)

Fig. 3. Zebra-crossing type precipitates observed in Al-Mg-Si-Mn casting alloys cast into PM (a) and HPDC (b)

from a solid solution initiating directly in the as-cast condition. Further investigations have to be carried out to reveal their crystalline structure and their role in the final determination of the mechanical properties of alloy. Therefore, the sequence of the precipitation process for Al-Mg-Si alloys could be modified by adding the first stage, i.e. decomposition of the solid solution (SS), formed during cooling after complete solidification. The most general expression for decomposition of supersaturated solid solution (SSSS) can be found in [14]. It starts when SSSS begins to decompose with solute clustering in the face centred cubic aluminium lattice. Then, the GP zones are formed followed by the formation of β'', β' and several other type of precipitates. Since the solid solution starts to decompose directly after casting, the order of phases formation could be corrected probably as follows: solid solution $\rightarrow$ clusters $\rightarrow$ GP $\rightarrow$ β'' (zebra-crossing) $\rightarrow$?. This can be one of the possible scenarios of the formation of zebra-crossing type precipitates. However, the structure and composition of these precipitates need to be studied in more details.

2.4. Effect of Cu and Zn

Additions of Cu and Zn lead to the considerable increase of UTS up to 350 MPa of Al-Mg-Si alloy (after addition of 0.60 wt.% Mn) [11]. Addition of 3.50 wt.% Zn results in a significant improvement of YS from 190 MPa for base alloys up to 250 MPa. The significant decrease of elongation was observed (down to 2.0%) while UTS remained at the level of 350 MPa. From a structural point of view the alloying of an Al-Mg-Si alloy with Zn promotes the formation of primary Zn-containing inter-metallic phase. It was reported that the Zn-containing phase could be identified as $Al_{13}Mg_5Zn$. Its particles are located at the boundaries of the α-Al solid solution.

Sometimes it can be observed between eutectic cells. It was also reported by Y. Milman et al. [12] that the Zn addition to the alloy cast into the permanent mould (PM) after heat treatment assured UTS up to 500 MPa (Zn content of 2.58 at.%), YS of 430 MPa and 1.0% elongation. The increase of mechanical properties is explained by the authors as due to the formation of the dispersive precipitates of η-$MgZn_2$ during heat treatment. However, the type of precipitates has to be studied in more detail because of the presence of a large number of alloying elements in α-Al may lead to the formation of a wide variety of particles. These may provide different contributions to the final mechanical properties of the alloy. An investigation of the effect of adding Cu on the mechanical properties of PM Al-Mg-Si-Mn casting alloy allowed one to establish that the presence of 0.20 at.% Cu led to a further increase in the mechanical properties of the alloy [12].

Investigations of the AlMg5.70Si2.85Mn0.61+Cu1.58+Zn2.23 alloy cast into PM showed that, in addition to the α-Al, eutectic (α-Al + Mg_2Si) and Mn-bearing phases, a new eutectic-type phase was formed during solidification (Fig. 4a,b). SEM/WDX analysis showed that its particles are enriched with Mg (14.80 wt.%), Cu (30.84 wt.%) and Zn (2.84 wt.%). Simultaneously, TEM/EDX measurements of the matrix composition revealed that the Mg content in α-Al decreases to 0.70−0.80 wt.% in comparison to 2.20 wt.% Mg in the alloy without the addition of Cu+Zn. These results showed that the addition of 1.5 wt.% Cu and 2.2 wt.% Zn caused formation of relatively large inter-metallics, adsorbing Mg directly from the solid solution. This effect should be considered rather undesirable. Therefore, the amount of Cu and Zn needs to be reduced for keeping the phase equilibria the same as it is in the quasi-binary section in the Al-Mg-Si system, in order to avoid formation of additional eutectic phases. From Figure 4b one can see that
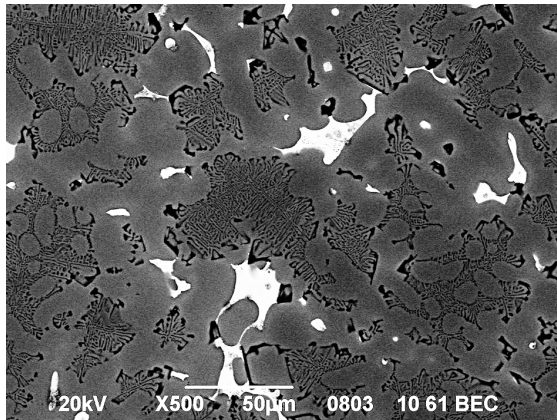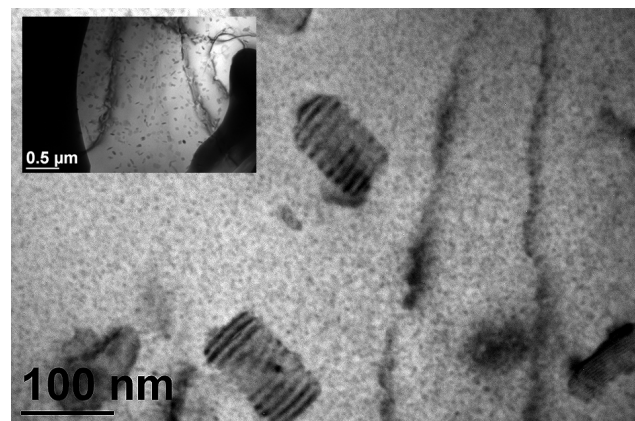
a) Microstructure of AlMg5.70Si2.85Mn0.61+Cu1.58+Zn2.23 alloy cast into PM
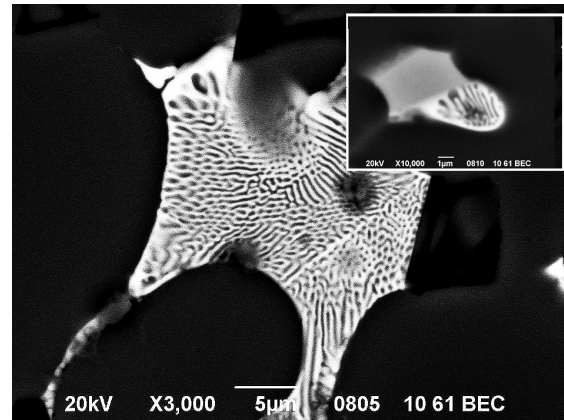
b) Morphology of eutectic-type intermetallic and adjoined Fe-bearing phase in AlMg5.70Si2.85Mn0.61+Cu1.58+Zn2.23 PM alloy
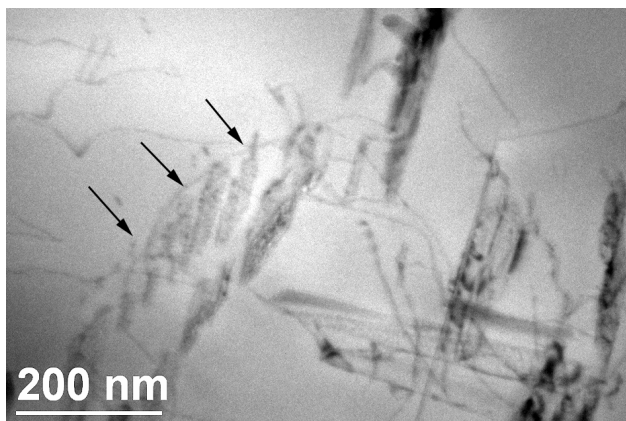
c) Bright field image of zebra-crossing type precipitates observed in AlMg6.20Si2.30Mn0.61Zn1.65 alloy cast into permanent mould (marked by arrow)

d) Bright field image of precipitates observed in AlMg5.70Si2.85Mn0.61+Cu1.58+Zn2.23 PM alloy after heat treatment

Fig. 4. Microstructure of AlMg5.70Si2.85Mn0.61+Cu1.58+Zn2.23 alloy cast into PM in as cast condition (a,b,c) and after heat treatment (d)

the eutectic-type phase is adjoined to another phase. This solid phase is a (Mn,Fe)-containing intermetallic having the composition: Si – 6.42 wt.%, Mn – 24.03 wt.%, Fe – 4.25 wt.% and Cu – 3.02 wt.%.

Similar to unalloyed based Al-Mg-Si material (Fig. 3a and b) in the dendrites of the α-Al solid solution zebra-crossing-type, precipitates have been clearly seen. The morphology of these precipitates was nearly identical to those in the Al-Mg-Si alloy without any addition. However, their number is much higher than that of unalloyed material (Fig. 3a). This means that the additional alloying enhanced the formation of such type precipitates. Therefore, a small addition of Cu and Zn could provide an opportunity for further improvement of the mechanical properties of Al-Mg-Si alloy yet achieved in as-cast condition.

Due to Cu and Zn additions, the formation of a new kind of the nano-scale precipitates occurred, as can be seen from Figure 4c. Precipitates are evenly distributed in the area of inter-dendritic eutectic, in the α-Al solid solution lamellas. Presumably they might be attributed to the η-MgZn$_2$ phase of the zebra-crossing-type. However, additional investigations have to be carried out to reveal and identify all types of inter-metallics which can form in Al-Mg-Si alloys with the addition of Zn and Cu.

2.5. Effect of Ni

It was reported by Yang et al. [13] that addition of Ni (in the range between 0.005 and 2.06 wt.%) causes an increase in the interlamellar spacing of eutectic (α-Al + Mg$_2$Si). In alloys subjected to HPDC, an increase of Ni content leads to the formation of two different intermetallic compounds. Very often in both types of Ni-containing, the phases presence of Fe, Mn and Si was revealed. However, no Al$_3$Ni phase has been found in the Al-Mg-Si alloy structure. It was also observed that an increasing of Ni content in HPDC AlMg5Si2Mn alloy

slightly enhanced YS simultaneously with significant reductions of elongation, from 17% for alloy without Ni down to 5% for an alloy with 2.06 wt.% Ni. Therefore, it could be supposed that the slight increase in a YS value below 10% achieved after Ni addition, was caused by Ni-rich intermetallic compound formation either at the α-Al grain boundaries or in the eutectic areas (α-Al) + (Mg_2Si).

2.6. Effect of Sc, Sc+Zr

Sc is considered as one of the principal additions to aluminium alloys due to its triple effect on the structure and properties of Al-based alloys. These include the nucleation effect of the primary Al_3Sc intermetallic phase, providing efficient grain refinement, modification of the eutectic structure in Al-Si alloy, and the precipitation hardening.

According to the binary Al-Sc phase diagram, particles of Al_3Sc should form during solidification of all alloys with Sc content higher than the 0.60 wt., during eutectic reaction Liq. = α-Al + Al_3Sc at a temperature range of 655−659°C [15]. A.F. Norman et al. [16] observed Al_3Sc in the centres of α-Al grains and concluded that they acted as their heterogeneous nuclei. They showed that the addition of Sc refines Al grains more effectively than well-known refiners such as Ti or Zr. This effect was mainly attributed to near-identical crystal structures of the Al_3Sc particles and the matrix phase. The primary particles of the Al_3Sc phase have faceted morphology and, as it was reported by Hyde et al. [17], they nucleated on the aluminium oxide particles. This nucleation mechanism was also recently confirmed by S. Zhou et al. [18] in the Al-5.0 wt.% Mg alloy with different Sc additions. Ramanaiah et al. [19] showed that the Sc addition provides a more effective grain refinement effect than that of Ti+B addition. However, U. Patakham et al. [20] stated that the grain refinement efficiency of Sc to the A356 alloy is lower than that of conventional Ti addition.

It was also stated that in Al-Si-Mg alloys different Al_3Sc intermetallic compounds may form that reduces the grain refining effect. It was shown that in high Si Al alloys ternary phase, $AlSc_2Si_2$ forms rather than Al_3Sc [8]. Simultaneously, the modification of eutectic (α-Al + Si) due to Sc addition was detected. Lim et al. [21] revealed slight grain refinement of A356 cast alloy together with the morphology of eutectic transformation (α-Al + Si), from coarse lamellar to the fine fibrous. The addition of 0.4 wt.% Sc led to an increase in the hardness of the A356 alloy up to 30% due to a combination of both effects of the refinement of α-Al grains and the eutectic modification allowed.

However, the high cost of Sc, and subsequently of binary Al-Sc master alloys limits the application of scandium additives to aluminium alloys, especially to cast materials. According to J. Røyset [22], in 2007 a price

of the Al-2.0 wt.% Sc master alloy was approximately 50 USD/kg.

It was established that the amount of Sc can be reduced by its combination with Zr. The formation of a ternary $Al_3(Sc_{1-x}Zr_x)$ intermetallic compound takes place instead of binary Al_3Sc and Al_3Zr [22], as during the Al_3Sc phase, a significant amount of Zr can solve. The ability of Al_3Sc and Al_3Zr primary particles to nucleate α-Al solutions was proven convincingly, while data concerning a similar effect of the ternary $Al_3(Sc_{1-x}Zr_x)$ particles were rather limited and sometimes controversial. However, the particles of $Al_3(Sc_{1-x}Zr_x)$ phase were observed inside the dendrite arm in the AlSi7Mg alloy after Sc+Zr addition. Based on the calculations of lattice parameters of $Al_3(Sc_{1-x}Zr_x)$ [23] it was stated that an increase in Zr content reduced both the lattice parameter of ternary $Al_3(Sc_{1-x}Zr_x)$ phase and its misfit with the lattice of α-Al. Also, in eutectic (α-Al + Si) the transition from plate-like to fine fibrous morphology took place after the addition of either Zr or Sc+Zr [23].

The first attempts to improve properties of the AlMg3Si1 casting alloy by adding Sc+Zr were performed by K. Eigenfeld et al. [24]. It was found that the AlMg3Si1+(Sc+Zr) alloy was the most promising candidate for application in the temperature range between 200 and 300°C.

Experimental investigations performed by authors showed that the structure of the Al-Mg-Si-Mn casting alloy can be effectively refined via complex additions of Sc+Zr to the melt. From the Figures 5a and 5b the primary $Al_3(Sc_{1-x}Zr_x)$ phase can be clearly seen in the centre of α-Al grain, which indicates the ability of this phase to nucleate the α-Al grains. The average size of the primary $Al_3(Sc_{1-x}Zr_x)$ phase particles was about 1.0−1.5 µm, comparable with previous results of others [23]. Besides α-Al grain refinement, more homogeneous distribution of alloying elements, fewer segregations, better feeding behaviour, more uniform distribution of porosity and lower surface roughness could be expected. Similar morphology of primary Al_3Sc particle was observed by J. Hyde et al. [26] after the cooling of Al-Sc alloy at a rate of approximately 100 K·s⁻¹.

The formation of a large fraction of primary intermetallics reduces the Sc or Sc+Zr content in α-Al solid solution, thus the formation of strengthening precipitates is limited. In the alloy under examination, the number of $Al_3(Sc_{1-x}Zr_x)$ particles was much higher than was necessary for fine equiaxed grain formation (*see* Fig. 5c, particles of $Al_3(Sc_{1-x}Zr_x)$ phase are marked by arrows). The primary $Al_3(Sc_{1-x}Zr_x)$ particles visible inside eutectic areas could generate a modifying effect, as the eutectic growth started from the surface of the $Al_3(Sc_{1-x}Zr_x)$ phase.

The distribution of Sc across the dendrite arm in the Al-Mg-Si-Mn casting alloy was carefully measured using TEM+EDX (Fig. 5d). The highest Sc content was 0.11 wt.%, whereas overall Sc content in the alloy is
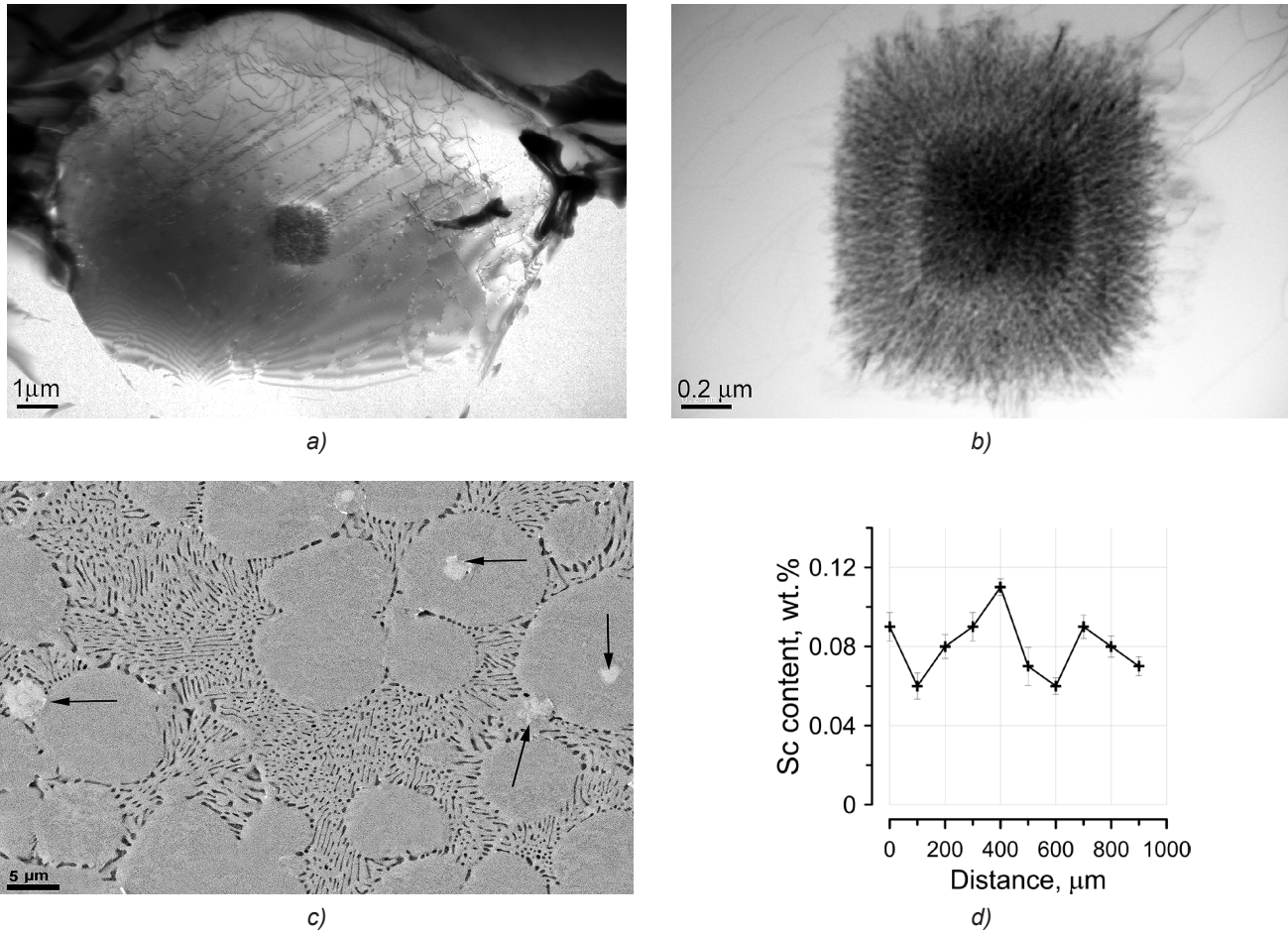
a)

b)

c)

d)

Fig. 5. Structure of Al-5.57 wt.% Mg-3.22 wt.%Si-0.64 wt.% Mn + (0.20 wt.%Sc+0.14 wt. %Zr) casting alloy: (a) bright field image of the α-Al grain, (b) morphology of $Al_3(Sc_{1-x}Zr_x)$ particle in the grain centre, (c) distribution of primary $Al_3(Sc_{1-x}Zr_x)$ particles in the alloy (marked by arrows), (d) distribution of Sc across dendrite arm

Table 3. Composition of α-Al solid solution at room temperature of different Al-Mg-Si-Mn casting alloys

Alloy	Composition of α-Al, wt.% (Al-balance)							
	Mg*	Si	Mn	Sc	Zr	Fe	Ti	Other
Base alloy (AlMg6.1Si2.9Mn0.7, no addition)	2.20	-	0.3	-	-	-	-	-
Addition of Li (AlMg6.1Si2.1Mn0.59+0.5wt.% Li)	2.5	-	0.5	-	-	-	-	-
Addition of Sc+Zr (AlMg6.2Si2.3Mn0.64+0.20wt.%Sc+0.09wt.% Zr)	1.5	-	0.3	0.1	-	-	-	-
A356 (AlSi7.2Mg0.35, no additions)	0.2	1.0	-	-	-	-	-	-
– average of 10 measurements								

0.20 wt.%, thus 0.09 wt.% Sc was bound in the primary Al_3Sc.

The most important role of Sc addition to the wrought alloys of Al-Cu, Al-Mg and Al-Li systems was the formation of nano-scale dispersoids of the type Al_3Sc (or in combination with Zr $Al_3(Sc_{1-x}Zr_x)$). They provided a strengthening effect due to dislocation movement blocking [15]. According to [21] the addition of 0.2 wt.% Sc to A356 casting alloy gives a slight increase of UTS from 91 to 108 MPa, while 0.4 wt.% of Sc was added, UTS decreased from 119 to 110 MPa in as-cast condition. This effect was most likely caused due to the formation of intermetallic compounds differing from Al_3Sc, withdrawing Sc from solid solution. The Al-Mg-Si alloys

seem to be more perspective to test effect of complex Sc+Zr addition on mechanical properties, especially at elevated temperatures [24]. Table 3 illustrates a composition of α-Al solid solutions in cast alloys of the Al-Mg-Si-Mn systems measured using TEM/EDX in as-cast condition.

Results in Table 3 show that when adding either Sc or Sc+Zr to alloy A356, some part of both elements could be bound into ternary silicide of the $AlSc_2Si_2$ type, reducing the amount of Sc+Zr available for the forming of strengthening phases.

As it was mentioned above, in the Al-Mg-Si-Mn alloys the Si content in the solid solution is very small – sometimes lower than the limit of detection – and no ternary Si-containing phases were observed. The simultaneous addition of Sc+Zr leads to decreases of Mg content in α-Al down to 1.52 wt.%. However, the fraction of zebra-crossing type precipitates in Sc+Zr containing alloys is somewhat higher than that in Al-Mg-Si-Mn base alloys cast into a permanent mould (Fig. 6). A.F. Norman et al. [16] observed precipitates of the similar shape and

distribution in both Al-Sc and Al-Cu-Sc alloys. Considering previous results of N. Blake and M.A. Hopkins [27], it was proposed that the mechanism for the formation of this type of precipitates, is discontinuous precipitation, often observed in Al-Sc alloys [22].

The driving force for grain boundary migration is a change in the alloy free energy during precipitation. As the grain boundary moves, it leaves behind a fan-shaped array of precipitates. However, the formation of discontinuous precipitates by moving grain boundaries cannot be an accurate description for casting materials. In Al-Mg-Si-Mn casting alloys containing Sc+Zr, annealing at 300°C for three hours leads to the formation of cubic-shaped fine precipitates (Fig. 7a,b). These are distributed in the α-Al solid solution (Fig. 7b) with narrow precipitation free zones close to Mg_2Si eutectic lamellae (Fig. 7a) as well as around primary particles (Fig. 7c). Simultaneously, the needle-shaped precipitates of β-Mg_2Si phase are also visible.

The detailed investigation of such type precipitates formed directly after cooling in a series of the Al-Mg-
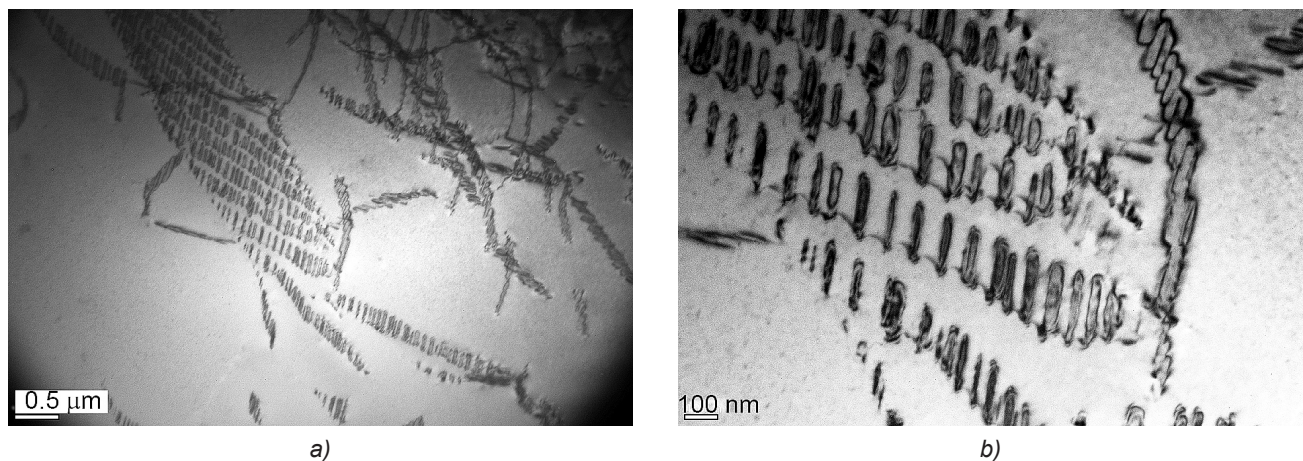

a) *b)*

Fig. 6. Bright field images of $Al_3(Sc_{1-x}Zr_x)$ zebra-crossing type precipitates formed in as-cast condition in AlMg6.2Si2.3Mn0.64+0.20 wt.%Sc+0.09 wt.% Zr alloy
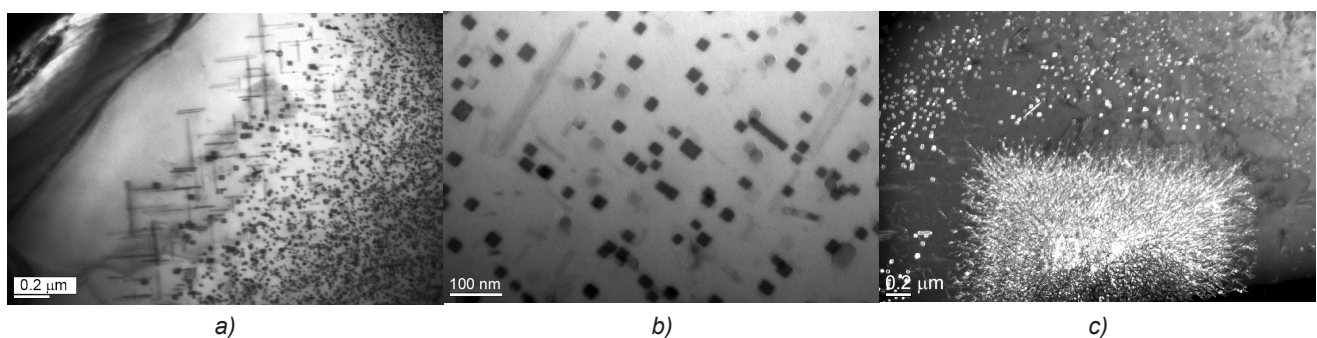

a) *b)* *c)*

Fig. 7. Micrographs of Al(Sc,Zr) precipitates in AlMg5Si2Mn casting alloy formed after addition of 0.20 wt.% Sc + 0.20 wt.% Zr and heat treatment: a) bright field image of $Al_3(Sc_{1-x}Zr_x)$ precipitates in the area close to (Al)+(Mg_2Si) eutectic lamellas, b) bright field image of morphology of $Al_3(Sc_{1-x}Zr_x)$ precipitates distributed in the α-Al, c) dark field micrograph of precipitation free zone around primary $Al_3(Sc_{1-x}Zr_x)$ particle

Si-Mn casting alloys with different elements additions clearly indicates that one of their sides is adjoined to dislocation. Their orientations were represented in the work [1]. The precipitates are lying in (100) planes, and their long axis is [010]. The dislocation has a Burgers vector of $\bar{b} = \pm \frac{1}{2}[10\bar{1}]$. It connects the plates on the right side in a curved line, which can be described by the average direction $[\bar{6}\,\bar{2}\,\bar{8}]$ or simplified [101]. So, the plates are not lying in one (100) plane but are shifted in the [100] and [001] direction. The dislocation forms a loop around each precipitate. Along the long side of the precipitate, the dislocation segment has a line vector of [010] and a Burgers vector of $\bar{b} = \pm \frac{1}{2}[10\bar{1}]$; i.e., it is an edge dislocation.

2.7. Effect of Li

Detailed reviews on the historical development and present state of the Al-Li alloys metallurgy, processes and applications can be found in [29−33]. In the book of L. Mondolfo [47] the solubility of Li in binary Al-Li alloys equals to (in wt.%): 4.3 at 602°C, 3.1 at 527°C, 2.2 at 420°C, 1.6 at 327°C, and 1.1 at 220°C. According to [32] the solubility of Li in Al at the eutectic temperature (above 600°C) is 4.2 wt.% and falls down to 0.4 wt.% at 200°C.

The next generation of Al-Li-X alloys are undergoing their implementation into the aerospace industry. The addition of both Li and Mg gives density reduction together with solid-solution strengthening and precipitation strengthening. The addition of both Cu and Ag provides solid solution and precipitation strengthening. The addition of Zn allows solid solution strengthening and corrosion resistance improvement. The addition of both Zr and Mn allows control of recrystallization course [31].

As an example, Alcoa 2060 alloy developed in 2011, contains (wt.%): 0.75 Li, 3.95 Cu, 0.85 Mg, 0.25 Ag, 0.11 Zr, 0.3 Mn, and 0.4 Zn. At this level of addition, the as-cast microstructure of alloy is single phase [34] which is appropriate for wrought alloys. During heat treatment, homogenisation, quenching and artificial ageing, supersaturated solid solution decomposes through the precipitation of numerous types of nanoscale precipitates. According to E. Starke [29], the number of possible precipitates which might be formed in an Al-Li-Cu alloy during ageing exceeds nine different types. The investigation presented in [35], showed that in the Al-2.5Li-2.0Mg-0.15Zr-0.12Ti alloy (UTS – 417 MPa and density – 2.52 g/cm^{-3}) the δ (AlLi) primary phase solidified in the dendrite-cell gaps and in the grain boundaries.

Following the advances of Al-Li-Cu and Al-Li-Mg wrought alloys, the idea to design Li-containing casting alloy still attracts researchers to design alloys with reduced density, and with the ability to be cast using conventional casting techniques. However, an increasing Li content leads to a decrease of fluidity. Due to the high reactivity of Li, the hydrogen content in Li-containing alloy was (1.05−1.23)×10^{-7} m^3·kg^{-1} whereas in the alloy without Li it was (0.19−0.60)×10^{-7} m^3 kg^{-1} [36]. For preventing Li-containing alloy from interacting with the atmosphere, it was proposed by V. Singh et al. [29] to use the casting ladle with protective gas covering.

Successful results of the development of Al-Li casting alloys and technology for their casting were obtained by R. Sauermann et al. [37]. They subjected the AlLi2.1Mg5.5+Zr0.15+Sc0.15 alloy to the novel Rheo-Container-Process. By using this technology designed for high-reactive materials, the alloy in a heat-treated condition achieved a UTS of 432 MPa with elongation to fracture at the level of 13%. Despite that, this result was a single event in the course of experiments, and it indicated the high potential of Li addition to improve the properties of specially designed casting alloys. Due to the reduced liquid phase content compared to conventional fully liquid casting, it is possible to remove some of the problems occurring with conventional processing of Al-Li alloys [38].

In the Al-Si alloys such as an A356 alloy [39−41] the Li addition leads to a simultaneous decreasing of strength and elongation. Nevertheless, Li on the level of 1.0−3.0 wt.% could lead to a change in the morphology of eutectic Si from flaky to fibrous [40]. In Al-12.0 wt.% Si containing 3.0 wt.% Li, formation of coarse ternary T-Li$_3$Al$_2$Si phase causes an important decrease in its mechanical properties. It was shown that the Li addition to Al-6.5Si-3.5Cu-1.0Fe (wt.%) alloy allows the modifications of the β-Al$_5$FeSi intermetallic compound. The microstructural effects of Li additions were more pronounced during a high cooling rate [42].

Information on the alloys of the Al-Mg-Si system containing Li is rather limited. One of the first attempts to characterize their structure was represented in the work of Li et al. [43]. Results of thermal analysis and metallographic studies showed that in the presence of Li, the area of stability of the two-phase structures of Al-Mg-Si, namely α-Al and (α-Al + Mg$_2$Si) was widened, which promoted high eutectic melting points and prevented the formation of ternary eutectics with a lower melting point. Research of V. Boyko [44] showed that the addition of 1.0 wt.% of Li to Al-6.7Mg-3.0Si-0.7Mn alloy keeps the eutectic melting temperature at 595°C, the same as it was detected for Al-6.5Mg-2.8Si-0.62Mn alloy without Li addition.

TEM investigation performed on the Li-containing Al-6.5Mg-2.8Si-0.62Mn PM alloy showed the appearance of zebra-crossing type precipitates observed in as-cast structures (Fig. 8a). It also demonstrated the formation of different types of precipitates in the same alloy after homogenisation at 570°C for 60 min, quenching and artificial aging at 175°C for 60 min. One can see that heat treatment resulted in the formation of at least four different types of precipitates (Fig. 8b). The needle-
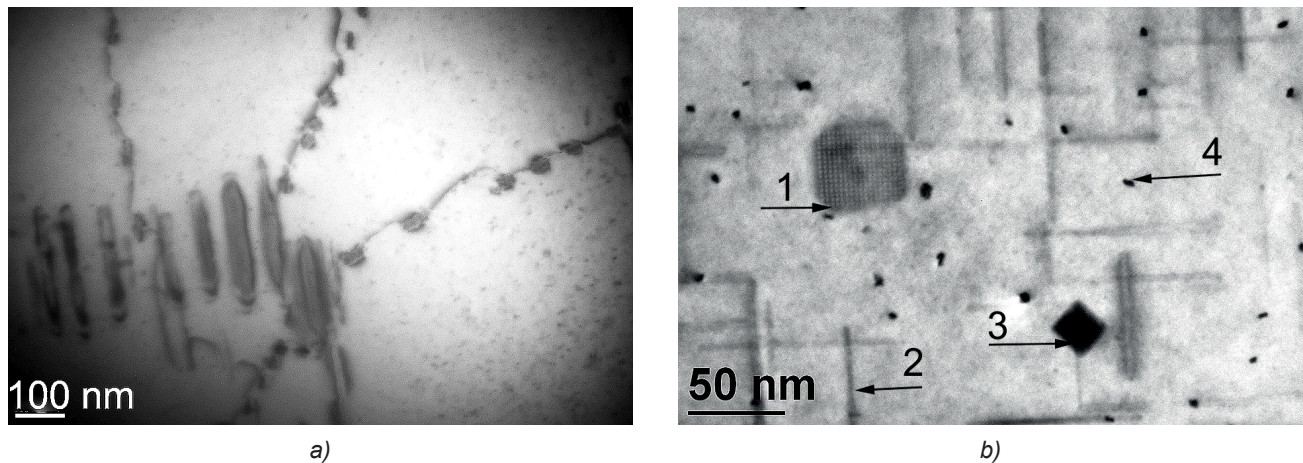
a)

b)

Fig. 8. Bright field images of zebra-crossing type precipitates formed in as-cast condition in Al-6.5Mg-2.8Si-0.62Mn PM alloy: (a) precipitates formed in the alloy after heat treatment, (b) alloy with Li addition

shaped particles in the β-Mg_2Si phase (marked as 2), while two types of cuboid precipitates (marked as 1 and 3) have been recognised as identical with black dots (marked as 4).

Summarising the existing information concerning the effect of Li on the structure and properties of Al-Mg-Si-Mn casting alloys, one can conclude that this material could form the basis for design of new Li-containing casting alloy possessing reduced density and good mechanical properties. It has been shown by V. Boyko et al. [1] that in as-cast condition the Brinell hardness as well as microhardness of α-Al of Al-5.3Mg-1.8Si-0.62Mn alloy (HB = 90 and $HV_{0.05}$ = 93.4 kgf/mm^2) is lower than that of Al-6.5Mg-2.8Si-0.62Mn+Li alloy (HB = 98 and $HV_{0.05}$ = 98.6 kgf/mm^2).

3. Summary

This review clearly shows the high potential of alloys based on the Al-Mg-Si-Mn system for expanding their application into casting practice, together with the possibility of increasing their properties. An additional alloying or use of micro-additions makes it possible to go from initial strengthening by a single type of precipitates into 'precipitation-zoo alloy' where the decomposition of the α-Al solid solution produces a set of precipitates of different types and composition. This leads to further improvement of strength and/or ductility or corrosion resistance of alloys. The summary of the effects of alloying elements is represented in Table 4.

Table 4. Summary of effect of different elements on structure of Al-Mg-Si-Mn-type casting alloys

Addition (range)	Resulting structural changes in as-cast condition (+/-)				Effect of heat treatment	
	Solid solution	Primary phase	Eutectic	Precipitates	Homogenisation	Aging
Mg (5.00−6.00 wt.%)	+	-	(α-Al + Mg_2Si)	zebra-crossing type	+supersaturation of α-Al solid solution	β-Mg_2Si
Si (1.50−2.00 wt.%)	-	-				
Mn (0.50−0.70 wt.%)	+	α-AlSiFeMn	(α-Al + Mg_2Si) + α-AlSiFeMn	zebra-crossing type	+supersaturation of α-Al solid solution	β-Mg_2Si, Mn-containing precipitates
Cu+Zn	+	eutectic-type large particles	(α-Al + Mg_2Si) + α-AlSiFeMnCu	zebra-crossing type	+supersaturation of α-Al solid solution	β-Mg_2Si, several types of precipitates
Sc+Zr (0.10−0.20 wt.% of both)	+	+	-	zebra-crossing type	supersaturation of α-Al solid solution	β-Mg_2Si Al(Sc,Zr), several types of precipitates
Li (0.5−1.0 wt.%)	+	-	-	-	supersaturation of (α-Al)solid solution	β-Mg_2Si several types of precipitates

References

1. Boyko V., E. Czekaj, M. Warmuzek, K. Mykhalenkov. 2017. "Effect of additional alloying and heat treatment on phase composition and morphology in Al-Mg-Si-type casting alloy". *Metallurgy and Foundry Engineering* 43 (3) : 219−239.

2. Prillhofer R., G. Rank, J. Berneder, H. Antrekowitsch, P.J. Uggowitzer, S. Pogatscher. 2014. "Property criteria for automotive Al-Mg-Si sheet alloys". *Materials* 7 (7) : 5047−5068.

3. Ji S., D. Watson, Z. Fan, M. White. 2012. "Development of a super ductile diecast Al-Mg-Si alloy". *Materials Science & Engineering A* A556 (30 October 2012) : 824−833.

4. Sanna F., A. Fabrizi, S. Ferraro, G. Timelli, P. Ferro, F. Bonollo. 2013. "Multiscale characterisation of AlSi9Cu3(Fe) die casting alloys after Cu, Mg, Zn and Sr addition". *La Metallurgia Italiana* (4) : 13−24.

5. Wuth M., H. Koch, A.J. Franke. 1999. Producing of steering wheels frames with an AlMg5Si2Mn-type alloy. In *Automotive Alloys*, ed. S.K. Das, 99−110. The Minerals, Metals and Materials Society.

6. Casarotto F., A.J. Franke, R. Franke. 2012. High-pressure die-cast (HPDC) aluminium alloys for automotive applications. In *Advanced materials in automotive engineering*, ed. J. Rowe. Woodhead Publishing Ltd.

7. Boyko V., E. Czekaj, M. Warmuzek, K. Mykhalenkov. 2017. "Design of new casting alloys of Al-Mg-Si-Mn system with alloying additions, its structure, and mechanical properties". *Metallurgy and Foundry Engineering* 43 (3) : 141−152.

8. Materials Science International Team MSIT®, Al-Mg-Si (Aluminium – Magnesium – Silicon). 2005. In *Light Metal Systems. Part 3. Landolt-Börnstein – Group IV Physical Chemistry (Numerical Data and Functional Relationships in Science and Technology)*, Vol. 11A3, eds. G. Effenberg, S. Ilyenko. Berlin, Heidelberg: Springer.

9. Mykhalenkov K., V. Boyko, T. Link. 2014. "Structure characterization and precipitation in two Al-Mg-Si-Mn casting alloys". *Metallurgy and Foundry Engineering* 40 (3) : 111−124.

10. Otarwanna S., C.M. Gourlay, H.I. Laukli, A.K. Dahle. 2009. "Microstructure formation in AlSi4MgMn and AlMg5Si2Mn high-pressure die castings". *Metallurgical and Materials Transactions A* 40 : 1645−1659.

11. Ji S., F. Yan, Z. Fan. 2015. "Development of a high strength Al–Mg_2Si–Mg–Zn based alloy for high pressure diecasting". *Materials Science & Engineering A* 626 (25 February 2015) : 165−174.

12. Milman Yu.V., T.N. Legka, N.P. Korzhova, V.V. Boyko, I.V. Voskoboynik, K.V. Mykhalenkov, N.M. Mordovets, Y.N. Podrezov Y.M. 2015. "Structure and mechanical properties of the casting high strength aluminum alloys of Al–Mg–Si ternary system alloyed by Zn and Cu / Электронная микроскопия и прочность материалов". 21 : 30−37.

13. Yang H., D. Watson, Y. Wang, S. Ji. 2014. "Effect of nickel on the microstructure and mechanical property of diecast Al–Mg–Si–Mn alloy". *Journal of Materials Science* 49 (24) : 8412−8422.

14. Ninive P. H., A. Strandlie, S. Gulbrandsen-Dahl, W. Lefebvre, C.D. Marioara, S.J. Andersen, J. Friis, R. Holmestad, O.M. Løvvik. 2014. "Detailed atomistic insight into the β´´ phase in Al–Mg–Si alloys". *Acta Materialia* 69 : 126−134.

15. Røyset J., N. Ryum. 2005. "Scandium in aluminium alloys". *International Materials Reviews* 50 (1) : 19−44.

16. Norman A.F., P.B. Prangnell, R.S. McEwen. 1998. "The solidification behavior of dilute aluminium-scandium alloys". *Acta Materialia* 46 (16) : 5715−5732.

17. Hyde K.B., A.F. Norman, P.B. Prangnell. 2000. "The growth morphology and nucleation mechanism of primary LI_2 Al_3Sc particles in Al-Sc alloys". *Material Science Forum* 331−337 : 1013−1018.

18. Zhou S., Z. Zhang, M. Li, D. Pan, H. Su, X. Du, P. Li, Y. Wu. 2016. "Effect of Sc on microstructure and mechanical properties of as-cast Al–Mg alloys". *Materials and Design* 90 (15 January 2016) : 1077−1084.

19. Ramanaiah N., K.S. Rao, B. Guha, K.P. Rao. 2005. "Effect of modified AA4043 filler on partially melted zone cracking of Al-alloy gas tungsten arc welds". *Science and Technology of Welding and Joining* 10 (5) : 591−596.

20. Patakham U., J. Kajornchaiyakul, C. Limmaneevichitr. 2012. "Grain refinement mechanism in an Al–Si–Mg alloy with scandium". *Journal of Alloys and Compounds* 542 (25 November 2012) : 177−186.

21. Lim Y.P., W.H. Yeo. 2014. "The effects of scandium on A356 aluminium alloy in gravity die casting". *Materials Research Innovations* 18 (6) : 395−399.

22. Røyset J. 2007. "Scandium in aluminium alloys overview: Physical metallurgy, properties and applications". *Metallurgical Science and Technology* 25 (2) : 11−21.

23. Xu C., W. Xiao, R. Zheng, S. Hanada, H. Yamagata, C. Ma. 2015. "The synergic effects of Sc and Zr on the microstructure and mechanical properties of Al–Si–Mg alloy". *Materials and Design* 88 : 485−492.

24. Eigenfeld K., A. Franke, S. Klan, H. Koch, B. Lenczowski, B. Pflege. 2004. "New developments in heat resistant aluminum casting materials". *Casting Plant and Technology International* 4 : 4−9.

25. Knipling K.E., D.C. Dunand, D.N. Seidman. 2006. "Criteria for developing castable, creep-resistant aluminum-based alloys – A review". *Zeitschrift für METALLKUNDE* 97 (2) : 246−264.

26. Hyde K.B., A.F. Norman, P.B. Prangnell. 2001. "The effect of cooling rate on the morphology of primary Al_3Sc intermetallic particles in Al-Sc alloys". *Acta Materialia* 49 (8) : 1327−1337.

27. Blake N., M.A. Hopkins. 1985. "Constitution and age hardening of Al-Sc alloys". *Journal of Materials Science* 20 (8) : 2861−2867.

28. Jeffris Z. 1959. *Paul Dyer Merica: A Biographical Memoir,* 227−240. Washington D.C.: National Academy of Sciences.

29. Starke E.A., Jr. 2014. Historical development and present status of aluminum-lithium alloys. In *Aluminum-Lithium Alloys. Processing, Properties, and Applications*, eds. N. Eswara Prasad, A.A. Gokhale, R.J.H. Wanhill. Elsevier Inc.

30. Belov N.A., D.G. Eskin, A.A. Aksenov. 2005. *Multicomponent phase diagrams. Applications for commercial aluminium alloys*. Elsevier Science.

31. Rioja R.J., J. Liu. 2012. "The evolution of Al-Li base products for aerospace and space applications". *Metallurgical and Materials Transactions A* 43 (9) : 3325−3337.

32. Costas L.P., R.P. Marshall. 1962. "The solubility of lithium in aluminum". *Transactions of the Metallurgical Society of AIME* 224.

33. Wenner S., C.D. Marioara, S.J. Andersen, M. Ervik, R. Holmestad. 2015. "A hybrid aluminium alloy and its zoo of interacting nano-precipitates". *Materials Characterization* 106 : 226−231.

34. Augustyn-Pieniążek J., H. Adrian, S. Rzadkosz, M. Choroszyński. 2013. "Structure and mechanical properties of Al-Li alloys as cast". *Archives of Foundry Engineering* 13 (2) : 5−10.

35. Saikawa S., K. Nakai, Y. Sugiura, A. Kamio. 1995. "Microstructures and mechanical properties of grain refined Al-Li-Mg casting alloy by containing Zr and Ti". *Journal of Japan Institute of Light Metals* 45 (7) : 385−390.

36. Saikawa S., K. Nakai, Y. Sugiura, A. Kamio. 1999. "Effect of hydrogen gas content on generation of porosity in Al/Li casting alloys". *Materials Transaction, JIM* 40 (1) : 57−63.

37. Sauermann R., B. Friedrich, T. Grimmig, M. Buenck, A. Bührig-Polaczek. 2006. "Development of Aluminium-Lithium alloys processed by the Rheo Container Process". *Solid State Phenomena* 116−117 : 513−517.

38. Sauermann R., B. Friedrich, T. Grimmig, M. Buenck, A. Bührig-Polaczek. 2006. "Development of Aluminum-Lithium alloy processed by the Rheo Container Process". *Solid State Phenomena* 116−117 : 513−517.

39. Tong C.H., L. Yao, C. Nieh, C. Chang, S. Hsu. 1987. "Castability of Al-Li-Mg and Al-Li-Mg alloys". *Journal de Physique Colloques* 48 (C3) : 117−122.

40. Zhao Z., Z. Qiao, C. Li, Q. Sun, P. Zhang, G. Wang. 2009. "Effect of Li on Al-Si alloys structure and properties". *Advanced Materials Research* 79−82 : 119−122.

41. Chen Z., C. Ma, P. Chen. 2012. "Eutectic modification of A356 alloy with Li addition through DSC and Miedema model". *Transactions of Nonferrous Metals Society of China* 22 (1) : 42−46.

42. Ashtari P., H. Tezuka, T. Sato. 2004. "Influence of Li addition on intermetallic compound morphologies". *Scripta Materialia* 51 (1) : 43−46.

43. Li S.-P., S.-X. Zhao, M.-X. Pan, D.-Q. Zhao, X.-C. Chen, O.M. Barabash. 2001. "Eutectic reaction and microstructural characteristics of Al (Li)-Mg_2Si alloys". *Journal of Materials Science* 36 : 1569−1575.

44. Boyko V. 2015. *Characterization of the structure and precipitation process in Al-Mg-Si and Al-Mg-Ge casting alloys*. PhD Thesis. TU-Berlin.

45. Hu Z., L. Wan, S. Wu, H. Wu, X. Liu. 2013. "Microstructure and mechanical properties of high strength die-casting Al–Mg–Si–Mn alloy". *Materials and Design* 46 : 451−456.

46. Hu Z., L. Wan, S. Lü, P. Zhu, S. Wu. 2014. "Research on the microstructure, fatigue and corrosion behavior of permanent mold and die cast aluminum alloy". *Materials and Design* 55 : 353−360.

47. Mondolfo L.F. 1979. *Aluminum alloys, structure and properties*. London: Butterworths.